Impact of neovascular age-related macular degeneration on eye-movement control during scene viewing: Viewing biases and guidance by visual salience

Antje Nuthmann, Miguel Thibaut, Thi Ha Chau Tran, Muriel Boucart

Impact of neovascular age-related macular degeneration on eye-movement control during scene viewing: viewing biases and guidance by visual salience

Antje Nuthmann[1], Miguel Thibaut[2], Thi Ha Chau Tran[2,3], and Muriel Boucart[2]

[1]Institute of Psychology, University of Kiel, Kiel, Germany
[2]University of Lille, Lille Neuroscience & Cognition, INSERM, Lille, France
[3]Ophthalmology Department, Lille Catholic Hospital, Catholic University of Lille, Lille, France

Antje Nuthmann http://orcid.org/0000-0003-3338-3434
Thi Ha Chau Tran https://orcid.org/0000-0001-9066-7092
Muriel Boucart https://orcid.org/0000-0001-7112-990X

Correspondence concerning this article should be addressed to Antje Nuthmann, University of Kiel, Institute of Psychology, Olshausenstr. 62, 24118 Kiel, Germany, or Muriel Boucart, Faculty of Medicine, Pôle Recherche, 1 place de Verdun, 59000 Lille, France, or via e-mail: nuthmann@psychologie.uni-kiel.de or muriel.boucart@chru-lille.fr.

Abstract

Human vision requires us to analyze the visual periphery to decide where to fixate next. In the present study, we investigated this process in people with age-related macular degeneration (AMD). In particular, we examined viewing biases and the extent to which visual salience guides fixation selection during free-viewing of naturalistic scenes. We used an approach combining generalized linear mixed modeling (GLMM) with a-priori scene parcellation. This method allows one to investigate group differences in terms of scene coverage and observers' well-known tendency to look at the center of scene images. Moreover, it allows for testing whether image salience influences fixation probability above and beyond what can be accounted for by the central bias. Compared with age-matched normally sighted control subjects (and young subjects), AMD patients' viewing behavior was less exploratory, with a stronger central fixation bias. All three subject groups showed a salience effect on fixation selection—higher-salience scene patches were more likely to be fixated. Importantly, the salience effect for the AMD group was of similar size as the salience effect for the control group, suggesting that guidance by visual salience was still intact. The variances for by-subject random effects in the GLMM indicated substantial individual differences. A separate model exclusively considered the AMD data and included fixation stability as a covariate, with the results suggesting that reduced fixation stability was associated with a reduced impact of visual salience on fixation selection.

233 words

keywords:
Macular degeneration; eye movements; naturalistic scenes; saliency; individual differences

1 Introduction

Patients suffering from advanced stages of age-related macular degeneration (AMD) have to rely on their peripheral vision to explore their surroundings and to perform tasks (see Verghese et al., 2021, for a review). Common complaints of patients with AMD (or more generally low vision) seeking visual rehabilitation are problems associated with reading, driving and face recognition (Cahill et al., 2005; Rubin, 2013; Taylor et al., 2016). Moreover, research has shown that AMD patients often suffer from fixation instability and poor oculomotor control (Crossland, Crabb, et al., 2011; Kumar & Chung, 2014). Therefore, it is perhaps unsurprising that few studies have investigated how AMD patients actively explore naturalistic scenes through eye movements. With the present work, we start to fill this gap by investigating eye guidance during free-viewing of real-world scenes in AMD patients as compared with normally sighted older and young adults. Primarily, we wanted to explore whether effects of visual salience on saccade target selection were preserved in patients with AMD.

When viewing a scene, we make sequences of saccades and fixations (Malcolm et al., 2016). Saccades are quick ballistic movements that bring the eyes to new parts of the scene. During fixations, the eyes are relatively still to allow visual processing of the scene stimulus. From a given fixation in the scene, there are many potential locations for the next fixation. Even without taking the current scene into account, fixation locations are not randomly selected. Among the regularities or "biases" in the manner in which we explore scenes, is the bias to fixate at or near the center of an image (central bias, Mannan et al., 1996; Tatler, 2007). Various factors contribute to the central bias (Rothkegel et al., 2017, for a review), among them strategic components. In particular, the center of the screen may be an optimal location for extracting information from scenes (Tatler, 2007).

The saccades we make during scene viewing are also biased: we make more horizontal eye movements than vertical ones, with oblique saccades being the least frequent (horizontal bias, Foulsham et al., 2008). The roots of the horizontal bias are still under investigation (Anderson et al., 2020; Foulsham & Kingstone, 2010). Given that the horizontal bias is already present in infants, it may be related to the asymmetry in the topography of human photoreceptors (Van Renswoude et al., 2016). According to another account, the distribution of image features may guide eye movements in a bottom-up manner toward the image horizon (Foulsham et al., 2008).

The saccade target selection process is also guided by the visual salience of the scene stimulus, in particular during free-viewing of scene images (Parkhurst et al., 2002; Peters et al., 2005). Guidance by visual salience means that the eyes are directed to scene regions based on image features generated in a bottom-up manner from the scene. These features, which tend to be correlated (Baddeley & Tatler, 2006; Nuthmann & Einhäuser, 2015), include luminance, contrast, edge density, and color (Mannan et al., 1996; Tatler et al., 2005). Different feature maps are combined in a saliency map (e.g., Itti et al., 1998), where brighter values indicate higher visual salience (see Figure 1b and c). Eye guidance by image features assumes that the eyes are directed to the most salient location in the map first, followed by an eye movement to the next most salient location, and so on. Due to the photographer's bias in scene composition, salience tends to be higher in the center of scenes (Tatler, 2007), calling for statistical methods that allow for assessing the independent contributions of visual salience and center bias to fixation selection in scenes (Nuthmann et al., 2017).

Saliency map models are models of visual attention rather than models of eye-movement control (see Frintrop et al., 2010, for a review), which may explain why most of them do not distinguish between visual salience in central vision as opposed to the periphery. Empirical eye-movement studies, on the other hand, have highlighted the importance of peripheral vision for the saccade target selection process. The importance of a given region of the visual field to a process or task can be assessed by implementing gaze-contingent artificial scotomas, which continuously remove (or strongly degrade) scene information in a selected region (e.g., David et al., 2019; Nuthmann, 2014).

For example, Nuthmann (2014) asked observers to search for a medium-sized target object in each scene. One of her six scotoma conditions simulated the absence of central vision. With only peripheral vision available, participants were able to direct their eyes to the object, and their initial landing positions on the object gave rise to a two-dimensional Gaussian distribution with a peak close to the center of the object (i.e., the Preferred Viewing Location, PVL, Nuthmann & Henderson, 2010). In other words, the PVL was preserved when observers' central vision was artificially impaired. This finding shows the importance of peripheral vision in fixation selection.

Moreover, Nuthmann (2014) used the eye-movement data to decompose the button-press search times into three phases representing particular sub-processes of search (Malcolm & Henderson, 2009). The data showed the following dissociation in behavior: Participants with a simulated *central* scotoma[1] were selectively impaired in verifying the identity of the target, but not locating it. In contrast, the same participants with a simulated *peripheral*

scotoma were selectively impaired in locating the target, but not identifying it (see also Nuthmann et al., 2021). The data suggest a central-peripheral dichotomy in which peripheral vision selects and central vision recognizes (Zhaoping, 2019).

AMD leads to a central scotoma due to which foveal or central analysis is impaired. As a result, the ability of people with AMD to correctly identify objects and scenes is reduced (Thibaut et al., 2015). However, patients' remaining peripheral vision has shown to be sufficient for object and scene categorization (Boucart et al., 2013; Tran et al., 2010). For example, Tran et al. (2010) showed that individuals with a central scotoma were able to categorize scenes displayed for 300 ms as natural/urban or indoor/outdoor with high accuracy (> 75% correct), even though their performance was below that of normally sighted controls. The results from categorization studies (see also Boucart et al., 2008; Tran et al., 2012) suggest that individuals with AMD are able to quickly recognize the overall meaning or "gist" of the scene.

In a more naturalistic setting, the rapid recognition of the scene's gist is supplemented by active scene exploration, for which people with AMD may adopt an eccentric viewing strategy. Eccentric viewing involves directing the eye such that the image falls onto still functioning parts of the retina. The region of retina used is referred to as the preferred retinal locus (PRL) or pseudo-fovea (Crossland, Engel, et al., 2011; Cummings et al., 1985; Timberlake et al., 1986).

In the present study, we asked participants to free-view images of naturalistic scenes. Thus, participants were given no specific instructions other than to look at the images. With our main analysis, we tested how "active" AMD patients' scene viewing behavior is, and how prone they are to the central fixation bias. Importantly, the analysis also allowed us to test whether image salience has an independent effect on fixation selection. We hypothesized that AMD patients explore fewer scene regions and exhibit a stronger center bias, due to problems with oculomotor control (see Verghese et al., 2021). Critically, assuming that the peripheral selection of the next fixation location follows similar guidance principles in AMD patients and normally sighted individuals, we expected to observe similar effects of image salience on fixation probability for the two subject groups. In a complementary analysis, we also investigated whether the horizontal bias was preserved in AMD patients.

We compared the eye-movement data of the AMD patients with data from age-matched, normally sighted older participants. Additionally, we included a group of young adults to dissociate the effects of pathology and normal ageing. Results from previous studies suggest that the effect of location-based visual salience on fixation probability is smaller for

older adults compared with young adults (Açik et al., 2010; Nuthmann et al., 2020). Moreover, it was found that young and older adults show similar levels of explorative viewing behavior (Açik et al., 2010) and no differences in central bias (Nuthmann et al., 2020).

For our main analysis, we used an approach combining generalized linear mixed modeling (GLMM) with a-priori scene parcellation (Nuthmann et al., 2017; Nuthmann et al., 2020). This method allows us to investigate group differences in terms of scene coverage, central bias and—crucially—the importance of image salience for fixation selection in scene viewing.

When conducting experiments, researchers are mainly interested in the average response to independent variables or predictor variables. Existing variability across subjects is typically treated as error variance (Cronbach, 1957), potentially obscuring differences between levels of an independent variable of interest (Vogel & Awh, 2008). However, this approach ignores many relevant sources of inter-subject variability, including the use of different strategies for the same task (Seghier & Price, 2018). Between-participant variance can differ considerably between populations. Groups of older adults often (but not always) show higher inter-subject variability than younger adults (Rabbitt, 1993; Shammi et al., 1998). Moreover, patient groups can have a high degree of heterogeneity (e.g., Wolfers et al., 2020).

When finding a group-level effect, it can be informative to explore the role played by factors associated with the individual. For example, in studies with AMD patients it is common to correlate a measure of their visual disability with their average score in a dependent variable of interest (e.g., Thibaut et al., 2016; Thibaut et al., 2015; Tran et al., 2010; Wiecek et al., 2012). In recent years, mixed-effects models have proved to be a particularly suitable tool for assessing individual differences (Kliegl et al., 2011; Rouder & Haaf, 2019). One particular advantage of mixed-effects models is that they allow one to make statistical inferences about experimental effects and individual differences on the basis of a single analysis. Therefore, a secondary aim of the present study is to demonstrate the use of GLMM for documenting reliable individual differences with regard to scene-viewing parameters in different subject groups.

2 Methods

2.1 Participants

The participants whose data we report in the present article took part in a larger study consisting of several tasks. The eye-tracking results from an object search task have been published elsewhere (Thibaut et al., 2020). The study was approved by the ethics committee for behavioral sciences at the University of Lille (N°EUDRACT 2010-101088-31) and was conducted in accordance with the tenets of the Declaration of Helsinki. All participants gave their written informed consent. The AMD patients and the age-matched control subjects were both recruited in the department of ophthalmology at the Saint-Vincent de Paul Hospital in Lille, France. The young observers were recruited among medical students and psychology students at the university.

Patients suffering from neovascular AMD with subfoveal involvement and with best corrected visual acuity (BCVA; i.e., acuity measured with subjective refraction) between 0.3 to 1 logMAR were included. They were treated with at least three monthly ranibizumab intravitreal injections prior to participating in the experiments. Clinical assessment included visual acuity measurement, funduscopy, and optical coherence tomography (OCT). BCVA was measured at a distance of 4 m using the ETDRS chart, which was converted to logMAR visual acuity.

Fluorescein angiography, indocyanine green angiography (ICGA), and spectral domain OCT (Heidelberg Retina Angiograph, HRA2; Heidelberg Engineering, Dossenheim, Germany) were used to confirm the diagnosis of neovascular AMD and to determine the size of the lesion (cf. Querques et al., 2012). With fluorescein angiography, the lesion area was defined as containing choroidal neovascularization, hemorrhages, scar tissue and serous pigment epithelial detachment. The ICG plaque was defined as an area of late hyperfluorescence seen in ICGA. The area of the lesion (mm^2) and the greatest linear diameter of the lesion (mm) were then measured by outlining the lesion using the Eye Explorer image analysis software (Heidelberg Engineering, Heidelberg, Germany). Microperimetry was not performed as several patients had very low vision (P4, P7, P10) or were too old (above 80 years) for such a long clinical test.

A French version of the Mini Mental State Examination (MMSE) was conducted to assess cognitive impairment in the AMD patients and in the age-matched normally sighted control subjects. We excluded participants with a history of neurologic or psychiatric disease,

cognitive impairment (MMSE < 25) or significant ocular diseases that might compromise oculomotor function.

Clinical assessment and experiments were performed during the same visit. The eye-tracking data from 17 patients diagnosed with AMD (14 women; mean age 78.2 ± 4.3 years) and 17 age-matched normally sighted controls (11 women; mean age 76.9 ± 7.2 years) were included for the present analyses. Note that 32 AMD patients were meant to be included, but the data from 15 patients had to be excluded due to excessive head movements, poor validation results for the calibration of the eye tracker, or data loss during eye-movement recordings (Thibaut et al., 2020). Additional data came from 17 young normally sighted controls (8 women; mean age 23.8 ± 2.5 years).

Eye movements were recorded monocularly. For patients with bilateral AMD, the eye with the best-corrected visual acuity was used. If both eyes had equal acuity, we selected one eye randomly. For young and older control subjects, their preferred eye was tracked. Note that viewing was monocular, with the non-tracked eye being occluded throughout calibrations and recordings.

Table 1 provides the individual demographic and clinical data for the AMD patients included in the study. The mean duration of the disease was three years, ranging from three to 98 months. Note that the variables describing patients' visual ability (visual acuity, greatest linear diameter of the lesion, and surface area of the lesion) are highly correlated with one another (Spearman's rank correlations: $r \geq 0.87$, $p < 0.001$). A few patients had training in eccentric viewing, to varying extents.

Insert Table 1 about here

2.2 Apparatus

Eye-tracking equipment by SensoMotoric Instruments (SMI, Teltow, Germany) was used. Eye movements were recorded with a tower-mount iViewX Hi-Speed eye tracker with a 350 Hz sampling rate (AMD patients, age-matched controls) and a portable RED-m eye tracker at 120 Hz (young participants). Both eye trackers offer comparable accuracy and precision. According to the manufacturer, the typical accuracy is 0.25 to 0.5° for the iViewX eye tracker, and 0.5° for the RED-m eye tracker. Eye-movement event detection took the differences in eye-tracker sampling rate into account.

The eye tracker was calibrated using a 5-point calibration procedure, followed by a 5-point calibration accuracy test. Subjects were asked to look at black discs (radius: 1°) that

appeared sequentially on the screen. The first calibration target was presented at the center of the screen, whereas the other ones were presented in random order in each of the four quadrants of the screen. The AMD patients fixated the calibration targets with their fovea or PRL (cf. Vullings & Verghese, 2021), see the Discussion section for additional considerations.

2.3 Design, stimuli, and procedure

The experiment was run using the Experiment Center software (SMI). First, participants' fixation stability was evaluated. To this end, participants were asked to fixate a black dot (radius: 1°) centrally displayed for 10 seconds on a light grey background. Afterwards, each participant free-viewed 20 color photographs of real-world outdoor scenes, 15 of which contained at least one person (see Figure 1a for an example). Each scene image was presented once for 10 s. Scene presentation was randomized across participants in each group. Each trial began with the presentation of a central cross for one second, which participants were instructed to fixate. Following a gap of 200 ms, the scene image was presented.

Scenes were displayed on a 17-inch Dell monitor with a screen resolution of 1280 × 1040 pixels (width × height). Scene images had an original resolution of 1024 × 683 pixels and were scaled up to 1280 × 854 pixels in the experiment. At a viewing distance of 60 cm, images subtended a visual angle of 36.3° × 29.5°. Images came with a small black framing. The analysis grid spanned the central 1200 × 800 pixels and thereby discounted the black surrounding.

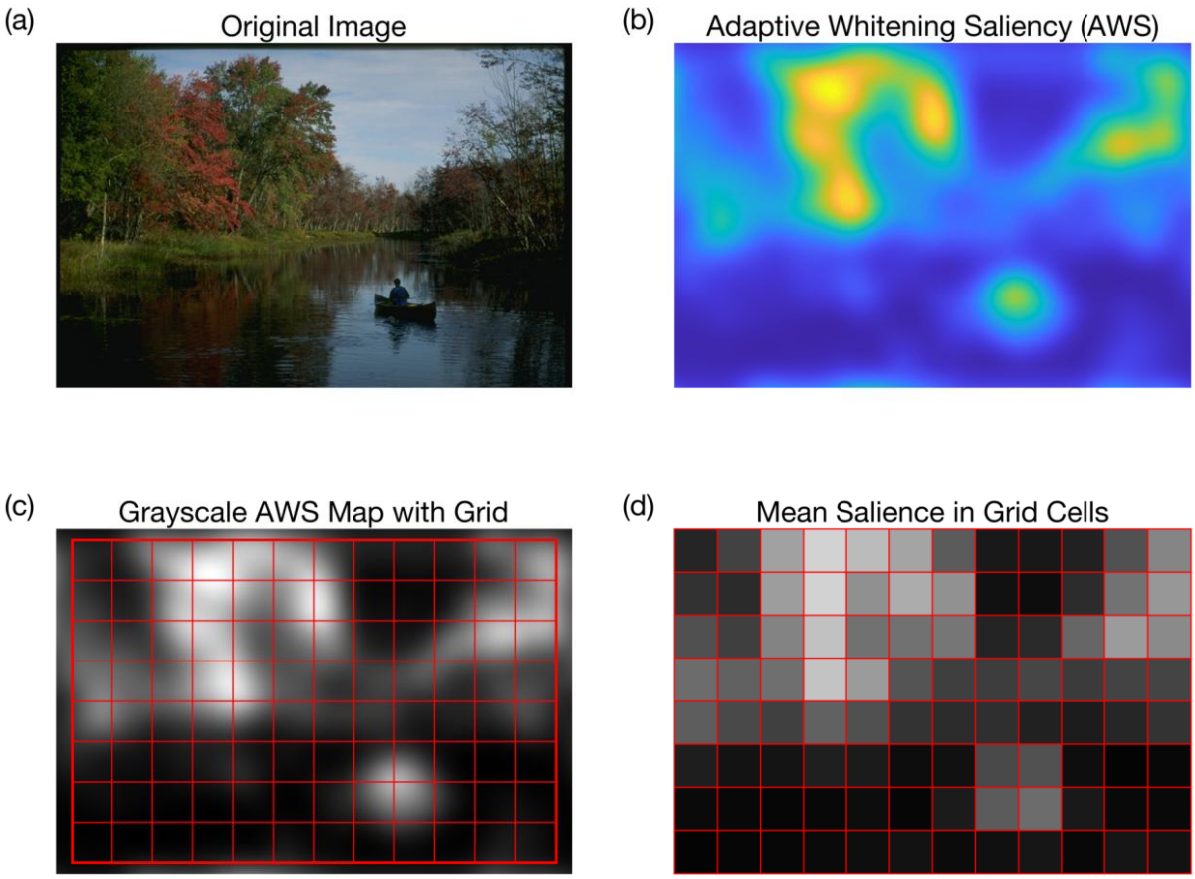

Figure 1. (a) One of the scene images used in the study. (b) A saliency map (Adaptive Whitening Saliency) for this image. (c) The same AWS map in grayscale, with the analysis grid overlaid in red. In panels (b) and (c), brighter regions indicate higher visual salience. (d) Mean salience values for the grid cells, color-coded using the gray colormap.

2.4 Data analysis

For a given participant, the gaze raw data from the scene viewing experiment were converted into a fixation sequence matrix and a saccade sequence matrix using the BeGaze software (SMI). For oculomotor event detection, the software's low-speed event detection method was used. With this method, the detector first searches for fixation events, after which saccade events are computed. To identify fixations, the detector uses a dispersion-based algorithm (cf. Salvucci & Goldberg, 2000), for which the default settings were used. In particular, the minimum fixation duration was set to 80 ms.

The fixation data were further processed and analyzed in MATLAB (The MathWorks, Natick, MA) and the R system for statistical computing. The figures were

created with MATLAB (Figure 1) or with the *ggplot2* (version 3.3.5, Wickham, 2016) and *cowplot* (Wilke, 2020) R packages.

Fixation probabilities and fixation counts were analyzed with generalized mixed-effects models (GLMMs). Continuous response variables, in particular fixation durations and saccade amplitudes, were analyzed using linear mixed-effects models (LMMs). Fixation durations were log-transformed prior to inclusion in the LMM (Nuthmann, 2017). The mixed-model analyses were conducted with the R package *lme4* (version 1.1-27.1, Bates et al., 2015), using the `glmer` function for GLMMs and the `lmer` function for LMMs. For LMMs, *p* values for fixated effects were obtained using Satterthwaite approximation as implemented in the *lmerTest* R package (version 3.1.3, Kuznetsova et al., 2017). For a technical introduction to mixed models in R, see Demidenko (2013). A tutorial is provided by Brown (2021).

2.4.1 Grid method

To assess the independent effect of visual salience on fixation probability, each scene image was parcellated into local image regions. As in previous research, we used a grid with equal-sized, square cells (Nuthmann & Einhäuser, 2015; Nuthmann et al., 2017; Nuthmann et al., 2020). How fine or coarse should the grid be? The problem with a very fine grid is that the trial-based observation matrix may contain too many zeros (cf. Nuthmann et al., 2017). The research question sets an upper bound for the grid cell size—it is implausible to investigate fixation guidance by visual salience with a very coarse grid. For the present analyses, we chose a 12 × 8 (width × height) parcellation (Figure 1c), yielding 96 quadratic cells, with each cell spanning 2.8° × 2.8° (100 × 100 pixels).

Next, we mapped the empirical eye-fixation data onto the scene analysis grid. We constructed an observation matrix based on the experimental design and the fixation data. The complete observation matrix would comprise 97,920 rows (3 subject groups × 17 subjects per group × 20 images × 96 grid cells per image). There were seven missing trials, reducing the observation matrix accordingly. In previous applications of the grid method, the grid cell on which the very first fixation in a given trial fell was excluded from analysis (e.g., Nuthmann & Einhäuser, 2015). For the present analysis, this grid cell was included if it received immediate refixations and/or later revisits. This procedure was adopted to guard against underestimating the central bias, in particular for AMD patients. Fixation probability was measured by a binary response variable: for a given subject and image, it was coded whether a given grid cell was fixated (1) or not (0).

2.4.2 Computation of saliency maps and central bias

Over the years, many different saliency models have been developed (Borji & Itti, 2013), for some of which the code is available publicly (e.g., Wloka et al., 2018). Following related work (Nuthmann et al., 2020), we used the Adaptive Whitening Saliency (AWS) Model (Garcia-Diaz et al., 2012). For each image, a corresponding saliency map was generated using code provided by the authors. The default parameters were used, with one exception: The output scaling factor (default value: 0.5) was set to 1.0 to compute saliency maps at full image resolution. The saliency map of each image was then normalized to the same range, arbitrarily chosen as [0,1] (Nuthmann et al., 2017). Supplementary Fig. 1 shows the mean normalized saliency map for the 20 scene images used in the study.

Local salience can be defined as the mean or the maximum (peak) over the saliency map's values within each grid cell. The correlation between mean and peak AWS across all grid cells from all images was very high, $r = 0.927$, $p < 0.001$. For the present analyses we chose the mean (see Figure 1d for a visualization), because it tends to be the more robust measure (Nuthmann et al., 2017; Nuthmann et al., 2020).

To account for observers' central bias of fixation, the GLMM included a central-bias predictor along with the salience predictor. How should the central-bias predictor be calculated? An intuitive solution is to determine the Euclidean distance from image center (e.g., Nuthmann & Einhäuser, 2015). The Euclidean distance-to-center variable is an isotropic measure, assuming equal spread of fixation positions in the horizontal and vertical dimensions. However, fixation positions in scene viewing often show a horizontal-vertical anisotropy (Clarke & Tatler, 2014). To decide about which central-bias variable to use, we took a data-driven approach (Nuthmann et al., 2017). In particular, we specified one-predictor GLMMs to test the seven central-bias predictors proposed by Nuthmann et al. (2017). For a given central-bias variable, one model considered the combined data from all three subject groups. Three additional models were run to analyze the data from each subject group separately. The more negative the standardized regression coefficient for the fixed effect central bias, the more variance is explained by the tested central-bias predictor (potentially leaving less variance to explain for the salience predictor). The numeric ranking of central-bias predictors differed across subject groups, but within a group the confidence intervals for the seven estimated central-bias effects overlapped. Further explorations revealed that AMD patients showed little anisotropy, compared with the other two groups. Numerically, the taxicab predictor performed best for the patient group. It was also chosen

for the present analyses because it was less sensitive to differences in anisotropy between groups, compared with other isotropic central-bias measures. The taxicab predictor was generated by calculating the distance between each grid cell center and the center of the image along the horizontal and vertical image axes:

$$C_{g,taxicab} = |x_g - x_c| + |y_g - y_c|. \quad (1)$$

2.4.3 Statistical analysis using mixed models

In our main analysis, we used generalized linear mixed models (Bolker et al., 2009; Jaeger, 2008) to model fixation probability in scenes for three different subject groups. The data were modeled at the level of individual observations (i.e., the zeros and ones). We used the logit transformation of the probability, which the `glmer` function uses by default for binary data. Using the logit link function means that parameter estimates are obtained on the log-odds or logit scale. This scale is symmetric around zero and ranges from negative to positive infinity. A logit of 0 corresponds to a probability of 0.5; negative log-odds indicate probabilities smaller than 0.5.

Mixed models incorporate both fixed-effects parameters and random effects. The GLMM included nine fixed effects (intercept, two main effects, six interaction coefficients). The two stimulus-related fixed effects were image salience and central bias. Stimulus-related input variables were measured within participants on a continuous scale. For the GLMM analyses, they were *z* transformed to a mean of 0 and a standard deviation of 1. Subject group is a categorical variable. To include subject group as predictor in the GLMM, contrast coding was used (see below). Differences between subject groups were tested through interactions between "subject group" and a given continuous predictor.

Random effects represent subjects' or items' deviations from the fixed-effect parameters; they are assumed to be normally distributed with a mean of 0 (Baayen et al., 2008). In our study design, the random factor "subject" is nested under "subject group", because each subject can only belong to one subject group. Subjects and scenes are crossed random effects, because every subject saw all 20 scene items.

Because we were particularly interested in individual differences, the GLMM was set up to include the "maximal" structure (Barr et al., 2013) for the random factor "subject". Thus, the random-effects structure comprised a by-subject random intercept, random slopes for central bias and salience, and three correlation parameters. This allowed us to explore the degree to which subjects differed in their responses above and beyond belonging to their subject group, which was modelled as a fixed effect. If there are genuine differences between

individuals, including by-subject random effects should lead to an improvement in model fit (see Staub, 2020).

Results from previous research on eye-movement control during scene viewing suggest that item variances are much larger than subject variances (Nuthmann & Einhäuser, 2015; Nuthmann et al., 2017). Therefore, the random-effects structure of the GLMM also included the maximal structure for the random factor "scene item".

Using Wilkinson notation (Wilkinson & Rogers, 1973), the model formula for the main GLMM reported in this article was:

Fixated ~ 1 + SubjectGroup + CentralBias + CentralBias:SubjectGroup + Salience + Salience:SubjectGroup + (1 + CentralBias + Salience | Subject) + (1 + CentralBias + Salience | Scene). (2)

3 Results

First, we report the results from the fixation stability test. Second, we characterize subjects' eye-movement behavior during scene viewing at a basic level. Third, we report results from our main analysis exploring whether individuals with AMD differ from age-matched control subjects (and young subjects) in terms of scene coverage and central bias and regarding the importance of image salience for fixation selection during scene viewing. Fourth, we report results from a complementary analysis, in which we explored another viewing bias; that is, the horizontal bias.

3.1 Fixation stability

Fixation stability was quantified by using the conventional method of calculating the Bivariate Contour Ellipse Area (BCEA) introduced by Steinman (1965) with parameters used by Crossland et al. (2004). A larger BCEA value is indicative of a less stable fixation. The results are presented in Figure 2 (for the AMD patients, see also Table 1). Our a priori hypotheses were as follows: fixation stability should be worse for AMD patients than for age-matched control subjects (Rohrschneider et al., 1995); moreover, fixation stability may be better for young than for older adults (Altemir et al., 2022). One-sided unpaired two-sample Wilcoxon tests confirmed these predictions. The BCEA (in minarc^2) for the AMD patients (*Mdn* = 9250, *IQR* = 10422) was significantly larger than the BCEA for the age-matched controls (*Mdn* = 3143, *IQR* = 5663), $W = 213$, $p = 0.009$. In contrast, the BCEA for the young adults (*Mdn* = 1363, *IQR* = 1389) was significantly smaller than the BCEA for the control group of older adults, $W = 61$, $p = 0.002$.

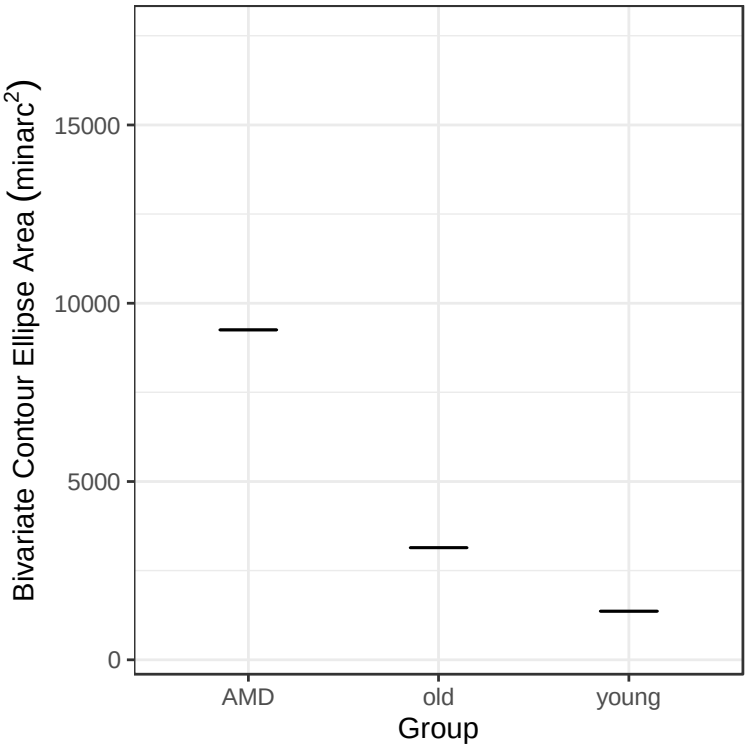

Figure 2. Fixation stability data for AMD patients, age-matched normally sighted subjects, and young adults. Each dot presents an individual participant's Bivariate Contour Ellipse Area (BCEA) value. The horizontal lines represent the medians for the three subject groups. Lower BCEA values indicate better fixation stability.

3.2 Basic Eye-Movement Measures

To provide a basic description of subjects' eye movements during scene viewing, we calculated the mean number of fixations per trial, along with mean fixation durations and saccade amplitudes (Table 2). Specifically, means or counts were calculated for each subject, and these were then averaged across subjects of a given group. The data were analyzed with mixed models, without prior averaging. Each model included the factor subject group as a fixed effect and random intercepts for subjects and scene items. To assess the effect of subject group, dummy coding (also referred to as treatment coding) was used, with the control group of old participants serving as the reference level. This coding created two contrasts, which allowed for testing whether there were any differences (a) between AMD patients and the control group or (b) between young and old participants.

The number of fixations per trial (count variable) was modeled using a Poisson GLMM with a log link function. The two contrasts were not significant (AMD - control: b = -

0.043, *SE* = 0.09, *z* = -0.48, *p* = 0.633; young - old: *b* = -0.036, *SE* = 0.09, *z* = -0.4, *p* = 0.691). Fixation duration and saccade amplitude (continuous variables) were analyzed with LMMs. For log-transformed fixation durations, the two planned contrasts were not significant (AMD - control: *b* = -0.083, *SE* = 0.099, *t* = -0.84, *p* = 0.406; young - old: *b* = 0.113, *SE* = 0.099, *t* = 1.14, *p* = 0.260). Saccade amplitudes were significantly reduced for AMD patients compared with age-matched controls, *b* = -1.423, *SE* = 0.4, *t* = -3.56, *p* < 0.001. Mean saccade amplitudes were not significantly different for young compared with old adults, *b* = 0.504, *SE* = 0.399, *t* = 1.26, *p* = 0.213. In summary, the main finding from these analyses is that AMD patients made saccades with shorter amplitudes than age-matched normally sighted subjects.

Insert Table 2 about here

3.3 GLMM results: Central bias and image salience

Next, we conducted a grid-based mixed-model analysis to assess effects of image salience on fixation selection, after controlling for subjects' tendency to look at the center of scene images. Using mixed modeling allows one to simultaneously investigate group differences and individual differences.

3.3.1 Group-level effects

To include the predictor subject group in the GLMM, a dummy-coding scheme was used. Consequently, the GLMM did not test main effects (i.e., average effects across the three subject groups) but simple effects; that is, effects for the reference group of old participants. Importantly, differences between the three subject groups were tested through interactions. For example, including the interaction between salience and subject group allowed for testing whether the salience effect was significantly different for either of the other two subject groups. The actual coefficient for the effect of salience in AMD patients (or young participants) is obtained by adding the simple effect coefficient and the relevant interaction coefficient. The GLMM results are summarized in Table 3, with the fixed-effects results depicted in Figure 3.

The first fixed effect in the GLMM is the intercept. It represents the overall fixation probability, describing how many different scene patches observers selected for fixation. The fixed effect for the model intercept characterizes the group of older adults: *b* = -2.049, *SE* = 0.122, *z* = -16.83, *p* < 0.001. Note that the logit value of -2.049 corresponds to a probability

of 0.114. The fact that the intercept was significantly different from zero has no interpretative meaning. Compared to the reference group of older adults, the intercept was significantly lower for AMD patients (b = -0.830, SE = 0.164, z = -5.04, $p < 0.001$), indicating that AMD patients fixated fewer scene patches than age-matched old observers. There was no significant difference between old and young adults (b = 0.291, SE = 0.162, z = 1.8, p = 0.072). The intercept coefficient for the AMD patients is the sum of the coefficient for the old subjects (-2.049) and the interaction coefficient (-0.830). The interaction coefficient is a difference score, describing the difference between AMD patients and old subjects. Figure 3a provides a visualization.

The central-bias predictor describes how fixation probability varies as a function of distance from scene center. A significant negative slope for the reference group (older adults) captures the well-known central bias (Mannan et al., 1996; Tatler, 2007); that is, fixation probability linearly decreased with increasing distance from scene center (b = -0.772, SE = 0.094, z = -8.18, $p < 0.001$). Compared to the reference group of older adults, the central-bias slope was significantly more negative for AMD patients (b = -0.534, SE = 0.128, z = -4.16, $p < 0.001$) and less negative for young adults (b = 0.256, SE = 0.126, z = 2.03, p = 0.043). Thus, the central bias was most pronounced for AMD patients, who showed an increased tendency to fixate central regions of the image. The central bias was weakest for young adults, with older adults in between.

Importantly, our GLMM based grid cell analysis allowed for assessing to what degree image salience influences fixation selection above and beyond a general preference for fixating the center of the image. For the reference group (older adults) there was a significant positive fixed effect for AWS, which means that fixation probability increased with increasing image salience of the image regions (b = 0.245, SE = 0.072, z = 3.40, p = 0.001). Young adults showed a significantly stronger effect of image salience than older adults (b = 0.25, SE = 0.079, z = 3.17, p = 0.002), which is in agreement with previous research (Açik et al., 2010; Nuthmann et al., 2020). Interestingly, there was no significant difference between AMD patients and older adults (b = -0.008, SE = 0.08, z = -0.1, p = 0.923).

Insert Table 3 about here

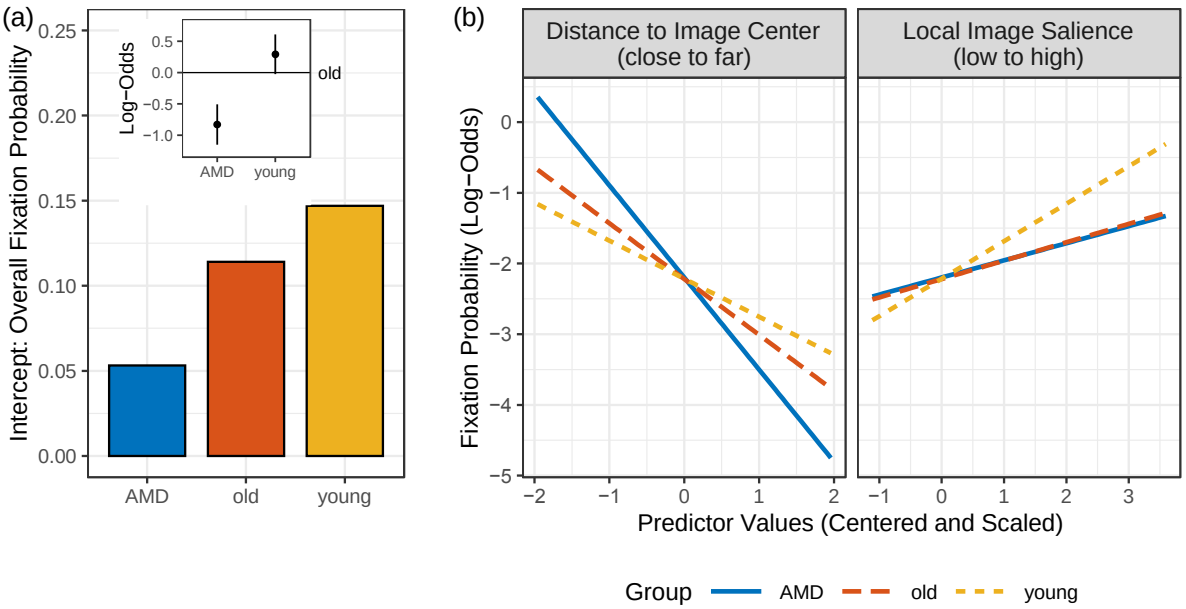

Figure 3. Fixed-effects results from the grid GLMM fitting fixation probability during scene viewing for AMD patients, old normally sighted control subjects, and young subjects. (a) Intercept, representing the overall fixation probability (converted from log-odds to probabilities). The brown bar depicts the intercept for the old subjects (reference group). The inset plot shows two difference scores: the difference between AMD patients and old subjects (AMD – old) and the difference between young and old subjects (young – old), with the error bars depicting 95% confidence intervals. Accordingly, the intercept for the AMD patients (blue bar) and/or young subjects (yellow bar) is derived by summing the simple effect coefficient for the old subjects and the respective difference score. (b) Predicted partial effects of central bias (left) and image salience (right) on fixation probability in log-odds scale for AMD patients (blue solid line), age-matched normally sighted subjects (brown long-dashed line), and young adults (yellow dashed line). The predictions were generated with the `keepef` function from the *remef* R package (Hohenstein & Kliegl, 2020).

To test the generalizability of results, a number of control analyses were performed. First, local salience was defined as the grid cell's peak salience rather than its mean salience. Second, the binary response variable (1 fixated, 0 not fixated) was replaced with fixation counts, which were modeled using a poisson GLMM with a log link function. Third, we repeated all analyses with a coarse 6 × 4 grid. The qualitative pattern of results did not change.[2]

3.3.2 Individual differences

The GLMM was set up with the maximal random-effects structure to protect against Type I errors (Barr et al., 2013; Schielzeth & Forstmeier, 2009). However, by including by-subject and by-item random effects we can also account for individual differences and item effects (Nuthmann et al., 2017). Here, we will use the GLMM results to assess whether there were reliable individual differences, which we expected to be particularly pronounced among the AMD patients.

To recapitulate, by-subject random effects represent subjects' deviations from the fixed-effect parameters. Accordingly, the zero lines in Figure 4a represent the fixed-effect estimates. Specifically, the vertical broken line in both panels of Figure 4a represents the model intercept. The horizontal broken lines represent the central-bias effect (left panel) and the salience effect (right panel), respectively. The dots in Figure 4a depict the by-subject random effects, with different colors denoting different subject groups. The horizontal and vertical error bars depict 95% prediction intervals.

For all three variables of interest, there are quite a few subjects for which the prediction intervals do not include the zero line (Figure 4a). For some of the subjects, particularly AMD patients, the prediction intervals are entirely on opposite sides of the zero line. Thus, the graphs are suggestive of considerable individual differences.

To test whether the differences between individuals were statistically reliable, the maximal model (Table 3) was compared with two reduced models. In model 1, the by-subject random slope capturing the central bias and the two correlation parameters involving the central bias were removed. In model 2, the by-subject random slope capturing the salience effect and the two correlation parameters involving image salience were removed.

Likelihood ratio tests (LRT) were used to determine whether dropping a particular random effect from the maximal model led to a significantly worse fit of the model. The log-likelihood increases with goodness of fit. The Akaike Information Criterion (AIC, Akaike, 1974) corrects the log-likelihood statistic for the number of estimated parameters. The Bayesian Information Criterion (BIC, Schwarz, 1978) additionally corrects for the number of observations. The AIC and BIC both decrease as goodness of fit increases.

According to the LRT, model 1 provided a significantly worse goodness of fit than the maximal model (logLik $\Delta\chi^2(3) = 584.66$, $p < 0.001$); moreover, both AIC and BIC were larger for model 1 than for the maximal model (AIC: 68685 – 68106 = 579; BIC: 68855 – 68305 = 550).

Model 2 also provided a significantly worse goodness of fit than the maximal model (logLik $\Delta\chi^2(3) = 402.9$, $p < 0.001$), with both AIC and BIC being larger for model 2 than for the maximal model (AIC: 68503 – 68106 = 397; BIC: 68674 – 68305 = 369). Put the other way around, including by-subject random slopes (and the corresponding correlation parameters) in the maximal model led to an improvement in model fit. In summary, the model comparisons substantiate that there were genuine differences between individuals.

To obtain individual subject coefficients for a given variable of interest, we need to add the predictions for random effects to the fixed-effect estimate. In Figure 4b, the differently colored dots depict the individual coefficients for the 51 subjects from the three different subject groups. For the 17 AMD patients, represented by the blue dots, the subject numbers from Table 1 are additionally provided. Moreover, the colored horizontal and vertical lines represent the fixed-effect estimates for the three variables and three subject groups.

To reiterate, the central bias describes the phenomenon that fixation probability decreases with increasing distance from image center. Therefore, almost all subject coefficients for the central-bias predictor are negative (Figure 4b, left). The more negative the central-bias coefficient, the stronger the central bias. The intercept represents the overall fixation probability. A smaller by-subject intercept means that fewer scene patches were fixated, and this is associated with a stronger central fixation bias. The systematic relationship between intercept and central bias is particularly evident for the AMD patients, with some of them showing a particularly strong central bias.

The salience effect captures the observation that fixation probability tends to increase with increasing image salience. Therefore, most subject coefficients for the salience predictor are positive (Figure 4b, right). However, some of the individual coefficients are negative or close to zero, which means that salience had no impact on fixation selection for these subjects. For example, AMD patient 10 shows a relatively strong central bias and no salience effect. AMD patient 8, on the other hand, shows low scene coverage and a strong central bias, but an average salience effect.

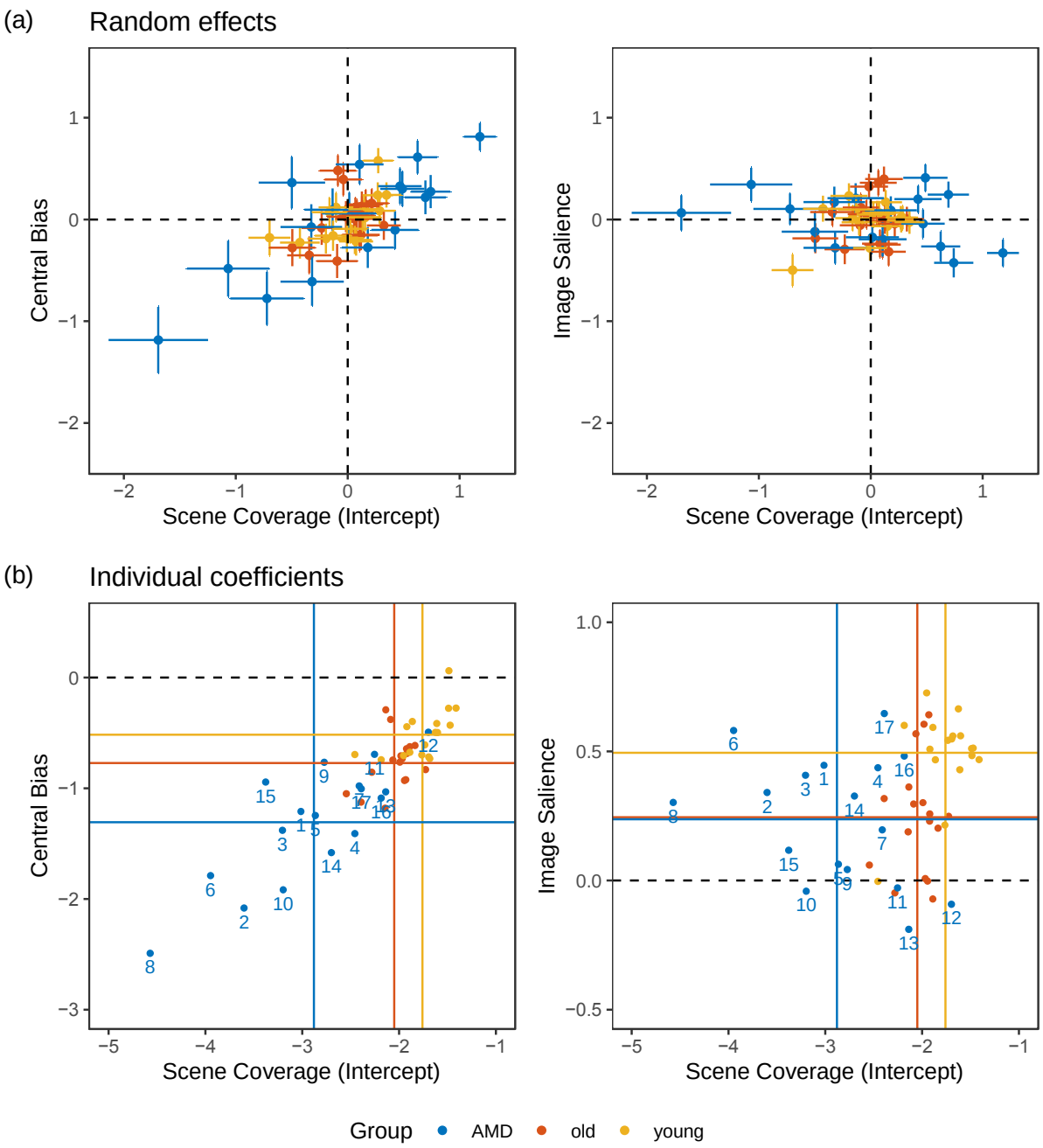

584

585 Figure 4. By-subject effects on fixation probability for the 51 subjects that took part in the
586 study. Scatterplots of the central-bias effect (left panels) and the salience effect (right panels)
587 against the intercept in the GLMM. The intercept represents the overall fixation probability; a
588 small by-subject intercept indicates that few scene patches were fixated (i.e., scene coverage
589 was low). In each panel, different colors denote subjects that belong to a given subject group
590 (blue: AMD, brown: age-matched old adults, yellow: young adults). (a) The conditional
591 modes of the distributions of random effects are shown by colored dots, given the
592 observations and evaluated at the parameter estimates. The horizontal and vertical error bars
593 depict 95% prediction intervals. (b) Individual subject coefficients; that is, the sum of fixed-

effect estimates and predictions for random effects. The colored vertical lines depict the fixed-effect estimates for the intercept in the GLMM for a given subject group. The colored horizontal lines depict the fixed-effect estimates for central bias (panel b, left) and salience (panel b, right) for a given subject group.

3.3.3 Inclusion of patient variables as fixed effects in the GLMM

A final question we considered is whether there is a systematic relationship between AMD patients' visual ability and indicators of fixation selection in scenes. An intuitive solution may be to compute correlations between measures of patients' visual ability (Table 1) and their GLMM subject coefficients (Figure 4b). Kliegl et al. (2011) point out that random effects for different subjects are not independent observations. For this reason, the authors advise not to use random effects (or individual coefficients) for further inferential statistics, and to refer to estimates of (G)LMM parameters instead. Accordingly, we evaluated the AMD patients' fixation data in another GLMM for which the fixed-effects structure comprised the central-bias and salience predictors, and also a "patient variable" and its interactions with central bias and salience. The model equation was as follows:

Fixated ~ 1 + CentralBias + Salience + PatientVariable + PatientVariable:CentralBias + PatientVariable:Salience + (1 + CentralBias + Salience | Subject) + (1 + CentralBias + Salience | Scene). (3)

For the predictor reflecting patients' visual ability we chose the surface area of the lesion (Table 1). We reasoned that a larger central scotoma may lead to a less effective use of peripheral vision and therefore to less exploratory viewing behavior and weaker guidance by visual salience. However, the main effect of surface area on fixation probability was not significant, $b = 0.142$, $SE = 0.197$, $z = 0.72$, $p = 0.472$. The interaction between surface area and central bias was also not significant, $b = 0.02$, $SE = 0.146$, $z = 0.14$, $p = 0.892$. The interaction between surface area and salience was not significant either, $b = -0.047$, $SE = 0.067$, $z = -0.7$, $p = 0.485$.

There was no systematic relationship between patients' scotoma size (surface area) and their BCEA value (Spearman's rank correlation: $r = 0.14$, $p = 0.600$), which is in agreement with previous research (e.g., Crossland, Culham, et al., 2004). Note that the results from reading studies suggest that higher BCEA values are associated with decreases in reading speed (e.g., Crossland, Culham, et al., 2004; Rubin & Feely, 2009). Therefore, we conducted an exploratory mixed-model analysis with predictors related to AMD patients'

BCEA values as fixed effects. This analysis allowed us to explore the relationship between patients' fixation stability and indicators of fixation selection. The main effect of fixation stability on fixation probability was not significant, $b = 0.135$, $SE = 0.198$, $z = 0.68$, $p = 0.494$. The interaction between fixation stability and central bias was also not significant, $b = 0.028$, $SE = 0.146$, $z = 0.19$, $p = 0.848$. However, there was a significant interaction between fixation stability and salience, $b = -0.155$, $SE = 0.056$, $z = -2.77$, $p = 0.006$, which means that higher BCEA values (indicating lower fixation stability) were associated with a smaller salience effect.[3]

3.4 Horizontal bias

When inspecting complex scenes, observers not only show a central bias, but also a horizontal bias; that is, a preference for horizontal over vertical and oblique saccades (Foulsham et al., 2008). In a complementary analysis, we therefore explored whether the horizontal bias was preserved in AMD patients.

The direction of a saccade was quantified as the angle between the horizontal plane and the line connecting the current fixation with the next fixation. For a given subject group, a polar histogram was constructed by sorting saccade angles from all observers into 36 equally spaced bins of 10°. The density histograms in Figure 5a show the expected horizontal bias. The saccade-angle distributions for AMD patients and age-matched control subjects showed no substantial differences. However, it appears that young adults made saccades along the horizontal plane (±5°) more frequently than older adults and AMD patients.

For statistical evaluation, the proportion of horizontal, vertical, and oblique saccades was calculated for each subject in a given group (cf. Van Renswoude et al., 2016). Saccades made along the 0° axis and the 180° axis (±30°) were classified as horizontal saccades, whereas saccades made along the 90° axis and the 270° axis (±30°) were classified as vertical saccades. Finally, saccades made along the 45°, 135°, 225°, and 315° axes (±15°) were classified as oblique saccades. Thus, each of the three directional categories (horizontal, vertical, oblique) covered the same angular range (i.e., 120°).

For a given subject group, about 50% of the saccades were classified as horizontal saccades (AMD patients: 48.7%, age-matched controls: 49.7%, young adults: 51.9%); see Figure 5b. The proportion of horizontal saccades did not differ between AMD patients and age-matched controls, $t(32) = -0.41$, $p = 0.688$. Using broadly defined categories, the proportion of horizontal saccades did not differ significantly between young and older adults

either, $t(32) = 0.9$, $p = 0.374$. None of the other two-sample t-tests indicated significant differences.

Figure 5. Analysis of the angular direction of saccades. (a) Distribution of saccade directions for AMD patients (blue solid line), age-matched normally sighted subjects (brown long-dashed line), and young adults (yellow dashed line). The polar histograms depict densities and were constructed using a bin size of 10°. The dots represent the bin centers. A 90° saccade angle denotes an upward saccade, 180° a leftward saccade, and 270° a downward saccade. The solid radial grid lines denote the cut-off points to classify horizontal, vertical, and oblique saccades; see text for additional details. (b) Proportion of horizontal, vertical, and oblique saccades for the three subject groups. Each dot presents an individual participant's proportion, and horizontal lines represent the mean. For a given subject group, the three mean proportions add up to 1.

4 Discussion

The purpose of this study was to investigate where and how AMD patients look at images of naturalistic scenes. Our analyses focused on viewing biases and the impact of visual salience. Compared with age-matched normally sighted subjects, AMD patients'

viewing behavior was less exploratory, with a stronger central fixation bias. Both subject groups showed an independent effect of image salience on fixation probability. The salience effect was not reduced in AMD patients, suggesting that eye guidance by visual salience was still intact. The horizontal bias was also preserved in the patient group.

In our scene viewing task, each trial started with the presentation of a central fixation cross, which meant that subjects started to explore the scene from its center. Successive fixation locations tend to be close to one another, introducing dependency (Barthelme et al., 2013). Therefore, the fixations that follow the initial, central fixation are also more likely located near the center of the scene. In our data, this showed as the well-known central fixation bias (e.g., Mannan et al., 1996), but note that a central tendency has also been observed for non-central initial fixation positions (Tatler, 2007).

In our experiment, subjects had 10 s to look at each scene image, giving them ample time to explore the whole image. An analysis of global eye-movement measures indicated that AMD patients made saccades with shorter amplitudes than age-matched control subjects (Table 2). In the grid GLMM analyses, this translated into a significantly reduced model intercept for the AMD patients, which means that they sampled significantly fewer scene patches than the control subjects (Table 3). Moreover, their central fixation bias was significantly stronger (Table 3, Figure 4). Finally, the results for the by-subject random effects showed a correlation between scene coverage and central bias: The fewer scene patches were selected for fixation, the stronger the central fixation bias (Table 3, Figure 4).

The unconstrained nature of our free-viewing task allowed subjects to adopt a viewing style that they deemed fit. AMD patients' less explorative viewing behavior may be due to impairments caused by their scotomata. Note that differences in viewing behavior between AMD patients and age-matched controls are likely to be task dependent. Thibaut et al. (2016) asked AMD patients to name pictures of real-world scenes that were presented for 2 s each and found that AMD patients "moved their eyes around more" (p. 88). Thus, AMD patients' explorativeness may depend on the demands imposed by the task at hand.

Despite the presence of a central scotoma, AMD patients were more likely to fixate high-salience than low-salience scene patches. This finding is not as counterintuitive as it may seem, given that selection for fixation is essentially a peripheral-vision task (see Ludwig et al., 2014; Nuthmann, 2014). Importantly, the salience effects for the patient group and the control group did not differ in size. At the same time, we found substantial individual differences, in particular in the patient group.

Evidence from previous studies suggests that the influence of low-level image features on fixation selection in scenes decreases with increasing age (Açik et al., 2010; Nuthmann et al., 2020). In agreement with this general result, we found that fixation probability was modulated by image salience to a greater extent for young adults than for older adults. We also found that the central bias was (somewhat) less pronounced for young adults, which is different from Nuthmann et al. (2020) who found no differences in central bias for young and older adults. Finally, the distributions of saccade directions indicated subtle differences between young and older adults, warranting further research.

In previous investigations, correlations between AMD patients' average scores in a dependent variable of interest and measures of their visual ability were assessed (e.g., Thibaut et al., 2016; Thibaut et al., 2015; Tran et al., 2010; Wiecek et al., 2012). In the present context, we could have generated the input for such correlation tests by fitting a separate generalized linear model to each subject's data. However, with this approach there is a risk of overfitting the data, because subjects with extreme values are "taken too seriously" (see Gelman & Hill, 2007). Instead, we ran a generalized linear mixed-effects model with by-subject random effects, which allowed us to make predictions for individual subjects in the light of the behavior of all other subjects. In such a model, unreliable between-subject variance in the effects is removed through shrinkage (Efron & Morris, 1977; Makowski et al., 2014; Rouder & Haaf, 2019). It is neither advised nor necessary to correlate the random effects for different subjects with other subject variables such as scotoma size (Kliegl et al., 2011). Instead, patient-related variables can be included as additional fixed-effect terms in the mixed model. Analyzing AMD patients' scene-viewing data this way, we observed a significant interaction between BCEA and visual salience. When fixation stability was low, the impact of visual salience on fixation selection was reduced. By contrast, the size of the lesion did not predict fixation selection in any way.

Eye tracking AMD patients is challenging. Calibrating a standard laboratory eye tracker requires subjects to look at a number of calibration targets with known coordinates (see https://youtu.be/69oriD6j1DI). Typically, the calibration targets are presented in random order to prevent subjects from anticipating the location of the next target, which may make them leave the current target before it disappears. Given that the calibration procedure requires subjects to saccade to single targets in peripheral vision, the targets need to be visually salient. However, the calibration procedure also requires subjects to fixate each target for a certain amount of time. If AMD patients fixate the target with the fovea, it is obscured by the scotoma. Therefore, some researchers have used a "wagon wheel" as

calibration target which is meant to help AMD patients with fixating the target's center of gravity with the fovea (González et al., 2006; Sullivan & Walker, 2015). Alternatively, patients with stable PRLs may use their PRLs rather than their foveae for calibration (see Gupta et al., 2018, for discussion).

For eye-tracking studies like ours, it is preferable if subjects approach the fixation task during calibration and the subsequent free-viewing task in similar ways. Therefore, during calibration we neither encouraged foveal fixation by using specifically designed calibration stimuli (Sullivan & Walker, 2015) nor did we specifically encourage the use of a PRL by instructing participants "to look at the target so that it could be seen" (Costela et al., 2017, p. 6074). As indicated in Sec. 2.2 above, we cannot say with certainty whether a given AMD subject used the fovea or a PRL to fixate the calibration targets. In the following, we discuss whether this has any bearing on the interpretation of our empirical findings.

In the context of scene viewing, the difference between using the fovea or a pseudo-fovea (PRL) can be described as prioritizing either "seeing" or "looking". If the patient adopts an eccentric viewing strategy, they will "see" what is at fixation, but their scotoma is likely to hide more eccentric scene content and therefore some of the candidate target locations for the next saccade. Conversely, if the patient does not use a pseudo-fovea, their scotoma will degrade scene information at fixation but leave more scene content visible in the periphery (and thus "to look for"). Either way, the peripheral selection of the target location for the next saccade should follow similar guidance principles as in normally sighted individuals. In agreement with this prediction, we found effects of visual salience on saccade target selection to be preserved in patients with AMD.

In principle, more complex scenarios can develop when patients change their fixation behavior, either between the calibration task and the free-viewing task, or within a given task. For example, Costela et al. (2017) compared gaze locations during free-viewing of dynamic scenes (i.e., videos) with the PRL used in a fixation task. The results suggested that people with central vision loss did not necessarily use the same PRL in the two tasks (see also Crossland, Crabb, et al., 2011). Such changes in fixation behavior can result in offsets between measured and actual gaze positions.

Note that our grid method is fairly robust in this regard. The scene patches or grid cells that we used for analysis were relatively large in size. Moreover, the mean salience of adjacent scene patches tends to be correlated (see Figure 1d). Finally, we assessed how explorative a subject's viewing behavior was by analyzing the number of scene patches observers selected for fixation. Thus, our analysis method tolerates reductions in accuracy

and precision, within limits. We note that other analyses commonly used to investigate eye guidance in scenes place higher demands on accuracy (e.g., Nuthmann, 2017). Therefore, it is important to continue developing methodologies for measuring the location of the PRL (e.g., Tarita-Nistor et al., 2015) along with eye-tracking technologies that explicitly address the use of a PRL (or sometimes multiple PRLs) instead of the fovea.

Acknowledgements

We thank Wolfgang Einhäuser for helpful discussions regarding the grid method.

References

Açik, A., Sarwary, A., Schultze-Kraft, R., Onat, S., & König, P. (2010). Developmental changes in natural viewing behavior: bottom-up and top-down differences between children, young adults and older adults. *Frontiers in Psychology*, *1*(11), Article 207. https://doi.org/10.3389/fpsyg.2010.00207

Akaike, H. (1974). A new look at the statistical model identification. *IEEE Transactions on Automatic Control*, *19*(6), 716-723. https://doi.org/10.1109/TAC.1974.1100705

Altemir, I., Alejandre, A., Fanlo-Zarazaga, A., Ortín, M., Pérez, T., Masiá, B., & Pueyo, V. (2022). Evaluation of fixational behavior throughout life. *Brain Sciences*, *12*(1), Article 19. https://www.mdpi.com/2076-3425/12/1/19

Anderson, N. C., Bischof, W. F., Foulsham, T., & Kingstone, A. (2020). Turning the (virtual) world around: Patterns in saccade direction vary with picture orientation and shape in virtual reality. *Journal of Vision*, *20*(8), Article 21. https://doi.org/10.1167/jov.20.8.21

Baayen, R. H., Davidson, D. J., & Bates, D. M. (2008). Mixed-effects modeling with crossed random effects for subjects and items. *Journal of Memory and Language*, *59*(4), 390-412. https://doi.org/10.1016/j.jml.2007.12.005

Baddeley, R. J., & Tatler, B. W. (2006). High frequency edges (but not contrast) predict where we fixate: A Bayesian system identification analysis. *Vision Research*, *46*(18), 2824-2833. https://doi.org/10.1016/j.visres.2006.02.024

Barr, D. J., Levy, R., Scheepers, C., & Tily, H. J. (2013). Random effects structure for confirmatory hypothesis testing: Keep it maximal. *Journal of Memory and Language*, *68*(3), 255-278. https://doi.org/10.1016/j.jml.2012.11.001

Barthelme, S., Trukenbrod, H., Engbert, R., & Wichmann, F. (2013). Modeling fixation locations using spatial point processes. *Journal of Vision*, *13*(12), Article 1. https://doi.org/10.1167/13.12.1

Bates, D. M., Mächler, M., Bolker, B. M., & Walker, S. (2015). Fitting linear mixed-effects models using lme4. *Journal of Statistical Software*, *67*(1), 1-48. https://doi.org/10.18637/jss.v067.i01

Bolker, B. M., Brooks, M. E., Clark, C. J., Geange, S. W., Poulsen, J. R., Stevens, M. H. H., & White, J.-S. S. (2009). Generalized linear mixed models: a practical guide for ecology and evolution. *Trends in Ecology & Evolution*, *24*(3), 127-135. https://doi.org/10.1016/j.tree.2008.10.008

Borji, A., & Itti, L. (2013). State-of-the-art in visual attention modeling. *IEEE Transactions on Pattern Analysis and Machine Intelligence*, *35*(1), 185-207. https://doi.org/10.1109/tpami.2012.89

Boucart, M., Despretz, P., Hladiuk, K., & Desmettre, T. (2008). Does context or color improve object recognition in patients with low vision? *Visual Neuroscience*, *25*(5-6), 685-691. https://doi.org/10.1017/s0952523808080826

Boucart, M., Moroni, C., Szaffarczyk, S., & Tran, T. H. C. (2013). Implicit processing of scene context in macular degeneration. *Investigative Ophthalmology & Visual Science*, *54*(3), 1950-1957. https://doi.org/10.1167/iovs.12-9680

Brown, V. A. (2021). An introduction to linear mixed-effects modeling in R. *Advances in Methods and Practices in Psychological Science*, *4*(1), 1-19. https://doi.org/10.1177/2515245920960351

Cahill, M. T., Banks, A. D., Stinnett, S. S., & Toth, C. A. (2005). Vision-related quality of life in patients with bilateral severe age related macular degeneration. *Ophthalmology*, *112*(1), 152-158. https://doi.org/10.1016/j.ophtha.2004.06.036

Clarke, A. D. F., & Tatler, B. W. (2014). Deriving an appropriate baseline for describing fixation behaviour. *Vision Research*, *102*, 41-51. https://doi.org/10.1016/j.visres.2014.06.016

Costela, F. M., Kajtezovic, S., & Woods, R. L. (2017). The preferred retinal locus used to watch videos. *Investigative Ophthalmology & Visual Science*, *58*(14), 6073-6081. https://doi.org/10.1167/iovs.17-21839

Cronbach, L. J. (1957). The two disciplines of scientific psychology. *American Psychologist*, *12*(5), 671-684. https://doi.org/10.1037/h0043943

Crossland, M. D., Crabb, D. P., & Rubin, G. S. (2011). Task-specific fixation behavior in macular disease. *Investigative Ophthalmology & Visual Science*, *52*(1), 411-416. https://doi.org/10.1167/iovs.10-5473

Crossland, M. D., Culham, L. E., & Rubin, G. S. (2004). Fixation stability and reading speed in patients with newly developed macular disease. *Ophthalmic and Physiological Optics*, *24*(4), 327-333. https://doi.org/10.1111/j.1475-1313.2004.00213.x

Crossland, M. D., Engel, S. A., & Legge, G. E. (2011). The preferred retinal locus in macular disease: toward a consensus definition. *Retina-the Journal of Retinal and Vitreous Diseases*, *31*(10), 2109-2114. https://doi.org/10.1097/IAE.0b013e31820d3fba

Crossland, M. D., Sims, M., Galbraith, R. F., & Rubin, G. S. (2004). Evaluation of a new quantitative technique to assess the number and extent of preferred retinal loci in macular disease. *Vision Research*, *44*(13), 1537-1546. https://doi.org/10.1016/j.visres.2004.01.006

Cummings, R. W., Whittaker, S. G., Watson, G. R., & Budd, J. M. (1985). Scanning characters and reading with a central scotoma. *American Journal of Optometry and Physiological Optics*, *62*(12), 833-843. https://doi.org/10.1097/00006324-198512000-00004

David, E. J., Lebranchu, P., Da Silva, M. P., & Le Callet, P. (2019). Predicting artificial visual field losses: A gaze-based inference study. *Journal of Vision*, *19*(14), Article 22. https://doi.org/10.1167/19.14.22

Demidenko, E. (2013). *Mixed models: Theory and applications with R* (2d ed.). John Wiley & Sons. https://doi.org/10.1002/9781118651537

Efron, B., & Morris, C. (1977). Stein's paradox in statistics. *Scientific American*, *236*(5), 119-127. https://doi.org/10.1038/scientificamerican0577-119

Foulsham, T., & Kingstone, A. (2010). Asymmetries in the direction of saccades during perception of scenes and fractals: Effects of image type and image features. *Vision Research*, *50*(8), 779-795. https://doi.org/10.1016/j.visres.2010.01.019

Foulsham, T., Kingstone, A., & Underwood, G. (2008). Turning the world around: Patterns in saccade direction vary with picture orientation. *Vision Research*, *48*(17), 1777-1790. https://doi.org/10.1016/j.visres.2008.05.018

Frintrop, S., Rome, E., & Christensen, H. I. (2010). Computational visual attention systems and their cognitive foundations: A survey. *ACM Transactions on Applied Perception*, *7*(1), Article 6. https://doi.org/10.1145/1658349.1658355

Garcia-Diaz, A., Leborán, C., Fdez-Vidal, X. R., & Pardo, X. M. (2012). On the relationship between optical variability, visual saliency, and eye fixations: A computational approach. *Journal of Vision*, *12*(6), Article 17. https://doi.org/10.1167/12.6.17

Gelman, A., & Hill, J. (2007). *Data analysis using regression and multilevel/hierarchical models*. Cambridge University Press.

González, E. G., Teichman, J., Lillakas, L., Markowitz, S. N., & Steinbach, M. J. (2006). Fixation stability using radial gratings in patients with age-related macular degeneration. *Canadian Journal of Ophthalmology-Journal Canadien d'Ophtalmologie*, *41*(3), 333-339. https://doi.org/10.1139/i06-019

Gupta, A., Mesik, J., Engel, S. A., Smith, R., Schatza, M., Calabrese, A., van Kuijk, F. J., Erdman, A. G., & Legge, G. E. (2018). Beneficial effects of spatial remapping for reading with simulated central field loss. *Investigative Ophthalmology & Visual Science*, *59*(2), 1105-1112. https://doi.org/10.1167/iovs.16-21404

Hohenstein, S., & Kliegl, R. (2020). *remef: Remove partial effects*. In *(R package version 1.0.7)*. https://github.com/hohenstein/remef/

Itti, L., Koch, C., & Niebur, E. (1998). A model of saliency-based visual attention for rapid scene analysis. *IEEE Transactions on Pattern Analysis and Machine Intelligence*, *20*(11), 1254-1259. https://doi.org/10.1109/34.730558

Jaeger, T. F. (2008). Categorical data analysis: Away from ANOVAs (transformation or not) and towards logit mixed models. *Journal of Memory and Language*, *59*(4), 434-446. https://doi.org/10.1016/j.jml.2007.11.007

Kliegl, R., Wei, P., Dambacher, M., Yan, M., & Zhou, X. (2011). Experimental effects and individual differences in linear mixed models: estimating the relationship between spatial, object, and attraction effects in visual attention. *Frontiers in Psychology*, *1*, Article 238. https://doi.org/10.3389/fpsyg.2010.00238

Kumar, G., & Chung, S. T. L. (2014). Characteristics of fixational eye movements in people with macular disease. *Investigative Ophthalmology & Visual Science*, *55*(8), 5125-5133. https://doi.org/10.1167/iovs.14-14608

Kuznetsova, A., Brockhoff, P. B., & Christensen, R. H. B. (2017). lmerTest Package: Tests in Linear Mixed Effects Models. *Journal of Statistical Software*, *82*(13), 1-26. https://doi.org/10.18637/jss.v082.i13

Loschky, L. C., Szaffarczyk, S., Beugnet, C., Young, M. E., & Boucart, M. (2019). The contributions of central and peripheral vision to scene-gist recognition with a 180º visual field. *Journal of Vision*, *19*(5), Article 15. https://doi.org/10.1167/19.5.15

Ludwig, C. J. H., Davies, J. R., & Eckstein, M. P. (2014). Foveal analysis and peripheral selection during active visual sampling. *Proceedings of the National Academy of Sciences of the United States of America*, *111*(2), E291-E299. https://doi.org/10.1073/pnas.1313553111

Makowski, S., Dietz, A., & Kliegl, R. (2014). Shrinkage—application and tutorial. https://doi.org/10.5281/zenodo.11172

Malcolm, G. L., Groen, I. I. A., & Baker, C. I. (2016). Making sense of real-world scenes. *Trends in Cognitive Sciences*, *20*(11), 843-856. https://doi.org/10.1016/j.tics.2016.09.003

Mannan, S. K., Ruddock, K. H., & Wooding, D. S. (1996). The relationship between the locations of spatial features and those of fixations made during visual examination of briefly presented images. *Spatial Vision*, *10*(3), 165-188. https://doi.org/10.1163/156856896X00123

Nuthmann, A. (2014). How do the regions of the visual field contribute to object search in real-world scenes? Evidence from eye movements. *Journal of Experimental Psychology: Human Perception and Performance*, *40*(1), 342-360. https://doi.org/10.1037/a0033854

Nuthmann, A. (2017). Fixation durations in scene viewing: Modeling the effects of local image features, oculomotor parameters, and task. *Psychonomic Bulletin & Review*, *24*(2), 370-392. https://doi.org/10.3758/s13423-016-1124-4

Nuthmann, A., Clayden, A. C., & Fisher, R. B. (2021). The effect of target salience and size in visual search within naturalistic scenes under degraded vision. *Journal of Vision*, *21*(4), Article 2. https://doi.org/10.1167/jov.21.4.2

Nuthmann, A., & Einhäuser, W. (2015). A new approach to modeling the influence of image features on fixation selection in scenes. *Annals of the New York Academy of Sciences*, *1339*(1), 82-96. https://doi.org/10.1111/nyas.12705

Nuthmann, A., Einhäuser, W., & Schütz, I. (2017). How well can saliency models predict fixation selection in scenes beyond central bias? A new approach to model evaluation using generalized linear mixed models. *Frontiers in Human Neuroscience*, *11*(10), Article 491. https://doi.org/10.3389/fnhum.2017.00491

Nuthmann, A., & Henderson, J. M. (2010). Object-based attentional selection in scene viewing. *Journal of Vision*, *10*(8), Article 20. https://doi.org/10.1167/10.8.20

Nuthmann, A., Schütz, I., & Einhäuser, W. (2020). Salience-based object prioritization during active viewing of naturalistic scenes in young and older adults. *Scientific Reports*, *10*(1), Article 22057. https://doi.org/10.1038/s41598-020-78203-7

Parkhurst, D., Law, K., & Niebur, E. (2002). Modeling the role of salience in the allocation of overt visual attention. *Vision Research*, *42*(1), 107-123. https://doi.org/10.1016/S0042-6989(01)00250-4

Peters, R. J., Iyer, A., Itti, L., & Koch, C. (2005). Components of bottom-up gaze allocation in natural images. *Vision Research*, *45*(18), 2397-2416. https://doi.org/10.1016/j.visres.2005.03.019

Querques, G., Tran, T. H. C., Forte, R., Querques, L., Bandello, F., & Souied, E. H. (2012). Anatomic response of occult choroidal neovascularization to intravitreal ranibizumab: a study by indocyanine green angiography. *Graefes Archive for Clinical and Experimental Ophthalmology*, *250*(4), 479-484. https://doi.org/10.1007/s00417-011-1831-5

Rabbitt, P. (1993). Does it all go together when it goes? *Quarterly Journal of Experimental Psychology Section a-Human Experimental Psychology*, *46*(3), 385-434. https://doi.org/10.1080/14640749308401055

Rohrschneider, K., Becker, M., Kruse, F. E., Fendrich, T., & Völcker, H. E. (1995). Stability of fixation: results of fundus-controlled examination using the scanning laser ophthalmoscope. *German Journal of Ophthalmology*, *4*(4), 197-202.

Rothkegel, L. O. M., Trukenbrod, H. A., Schütt, H. H., Wichmann, F. A., & Engbert, R. (2017). Temporal evolution of the central fixation bias in scene viewing. *Journal of Vision*, *17*(13), Article 3. https://doi.org/10.1167/17.13.3

Rouder, J. N., & Haaf, J. M. (2019). A psychometrics of individual differences in experimental tasks. *Psychonomic Bulletin & Review*, *26*(2), 452-467. https://doi.org/10.3758/s13423-018-1558-y

Rubin, G. S. (2013). Measuring reading performance. *Vision Research*, *90*, 43-51. https://doi.org/10.1016/j.visres.2013.02.015

Rubin, G. S., & Feely, M. (2009). The role of eye movements during reading in patients with age-related macular degeneration (AMD). *Neuro-Ophthalmology*, *33*(3), 120-126. https://doi.org/10.1080/01658100902998732

Salvucci, D. D., & Goldberg, J. H. (2000). Identifying fixations and saccades in eye-tracking protocols. *Proceedings of the Symposium on Eye Tracking Research and Applications*, 71-78. https://doi.org/10.1145/355017.355028

Schielzeth, H., & Forstmeier, W. (2009). Conclusions beyond support: overconfident estimates in mixed models. *Behavioral Ecology*, *20*(2), 416-420. https://doi.org/10.1093/beheco/arn145

Schwarz, G. (1978). Estimating the dimension of a model. *The Annals of Statistics*, *6*(2), 461-464. https://doi.org/10.1214/aos/1176344136

Seghier, M. L., & Price, C. J. (2018). Interpreting and utilising intersubject variability in brain function. *Trends in Cognitive Sciences*, *22*(6), 517-530. https://doi.org/10.1016/j.tics.2018.03.003

Shammi, P., Bosman, E., & Stuss, D. T. (1998). Aging and variability in performance. *Aging Neuropsychology and Cognition*, *5*(1), 1-13. https://doi.org/10.1076/anec.5.1.1.23

Staub, A. (2020). Do effects of visual contrast and font difficulty on readers' eye movements interact with effects of word frequency or predictability? *Journal of Experimental Psychology: Human Perception and Performance*, *46*(11), 1235-1251. https://doi.org/10.1037/xhp0000853

Steinman, R. M. (1965). Effect of target size luminance and color on monocular fixation. *Journal of the Optical Society of America*, *55*(9), 1158-1165. https://doi.org/10.1364/josa.55.001158

Sullivan, B., & Walker, L. (2015). Comparing the fixational and functional preferred retinal location in a pointing task. *Vision Research*, *116*, 68-79. https://doi.org/10.1016/j.visres.2015.07.007

Tarita-Nistor, L., Eizenman, M., Landon-Brace, N., Markowitz, S. N., Steinbach, M. J., & González, E. G. (2015). Identifying absolute preferred retinal locations during binocular viewing. *Optometry and Vision Science*, *92*(8), 863-872. https://doi.org/10.1097/opx.0000000000000641

Tatler, B. W. (2007). The central fixation bias in scene viewing: Selecting an optimal viewing position independently of motor biases and image feature distributions. *Journal of Vision*, *7*(14), Article 4. https://doi.org/10.1167/7.14.4

Tatler, B. W., Baddeley, R. J., & Gilchrist, I. D. (2005). Visual correlates of fixation selection: effects of scale and time. *Vision Research*, *45*(5), 643-659. https://doi.org/10.1016/j.visres.2004.09.017

Taylor, D. J., Hobby, A. E., Binns, A. M., & Crabb, D. P. (2016). How does age-related macular degeneration affect real-world visual ability and quality of life? A systematic review. *BMJ Open*, *6*(12), Article e011504. https://doi.org/10.1136/bmjopen-2016-011504

Thibaut, M., Boucart, M., & Tran, T. H. C. (2020). Object search in neovascular age-related macular degeneration: the crowding effect. *Clinical and Experimental Optometry*, *103*(5), 648-655. https://doi.org/10.1111/cxo.12982

Thibaut, M., Delerue, C., Boucart, M., & Tran, T. H. C. (2016). Visual exploration of objects and scenes in patients with age-related macular degeneration. *Journal Français d'Ophtalmologie*, *39*(1), 82-89. https://doi.org/10.1016/j.jfo.2015.08.010

Thibaut, M., Tran, T. H. C., Delerue, C., & Boucart, M. (2015). Misidentifying a tennis racket as keys: object identification in people with age-related macular degeneration. *Ophthalmic and Physiological Optics*, *35*(3), 336-344. https://doi.org/10.1111/opo.12201

Timberlake, G. T., Mainster, M. A., Peli, E., Augliere, R. A., Essock, E. A., & Arend, L. E. (1986). Reading with a macular scotoma. I. Retinal location of scotoma and fixation area. *Investigative Ophthalmology & Visual Science*, *27*(7), 1137-1147.

Tran, T. H. C., Despretz, P., & Boucart, M. (2012). Scene perception in age-related macular degeneration: the effect of contrast. *Optometry and Vision Science*, *89*(4), 419-425. https://doi.org/10.1097/OPX.0b013e31824c3a21

Tran, T. H. C., Rambaud, C., Despretz, P., & Boucart, M. (2010). Scene perception in age-related macular degeneration. *Investigative Ophthalmology & Visual Science*, *51*(12), 6868-6874. https://doi.org/10.1167/iovs.10-5517

Van Renswoude, D. R., Johnson, S. P., Raijmakers, M. E. J., & Visser, I. (2016). Do infants have the horizontal bias? *Infant Behavior & Development*, *44*, 38-48. https://doi.org/10.1016/j.infbeh.2016.05.005

Verghese, P., Vullings, C., & Shanidze, N. (2021). Eye movements in macular degeneration. *Annual Review of Vision Science*, *7*, 773-791. https://doi.org/10.1146/annurev-vision-100119-125555

Vogel, E. K., & Awh, E. (2008). How to exploit diversity for scientific gain: Using individual differences to constrain cognitive theory. *Current Directions in Psychological Science*, *17*(2), 171-176. https://doi.org/10.1111/j.1467-8721.2008.00569.x

Vullings, C., & Verghese, P. (2021). Mapping the binocular scotoma in macular degeneration. *Journal of Vision*, *21*(3), Article 9. https://doi.org/10.1167/jov.21.3.9

Wickham, H. (2016). *ggplot2: Elegant graphics for data analysis* (2d ed.). Springer. https://doi.org/10.1007/978-3-319-24277-4

Wiecek, E., Jackson, M. L., Dakin, S. C., & Bex, P. (2012). Visual search with image modification in age-related macular degeneration. *Investigative Ophthalmology & Visual Science*, *53*(10), 6600-6609. https://doi.org/10.1167/iovs.12-10012

Wilke, C. O. (2020). *Cowplot: Streamlined plot theme and plot annotations for 'ggplot2'*. In *(R package version 1.1.1).* https://CRAN.R-project.org/package=cowplot

Wilkinson, G. N., & Rogers, C. E. (1973). Symbolic description of factorial models for analysis of variance. *The Royal Statistical Society Series C-Applied Statistics*, *22*(3), 392-399. https://doi.org/10.2307/2346786

Wloka, C., Kunić, T., Kotseruba, I., Fahimi, R., Frosst, N., Bruce, N. D. B., & Tsotsos, J. K. (2018). SMILER: Saliency model implementation library for experimental research. *arXiv preprint*. https://doi.org/10.48550/arXiv.1812.08848

Wolfers, T., Beckmann, C. F., Hoogman, M., Buitelaar, J. K., Franke, B., & Marquand, A. F. (2020). Individual differences v. the average patient: mapping the heterogeneity in ADHD using normative models. *Psychological Medicine*, *50*(2), 314-323. https://doi.org/10.1017/s0033291719000084

Zhaoping, L. (2019). A new framework for understanding vision from the perspective of the primary visual cortex. *Current Opinion in Neurobiology*, *58*, 1-10. https://doi.org/10.1016/j.conb.2019.06.001

Footnotes

[1] Visual cognition researchers typically consider central vision to be from 0° to 5° eccentricity; everything beyond 5° is peripheral vision (Loschky et al., 2019).

[2] There was one exception: When using the binary response variable and a 6 × 4 grid, the model intercept was significantly larger for young compared with old subjects. In our main analysis, this difference was not significant (Table 3, Figure 3a).

[3] In both of these additional GLMMs, the fixed-effect coefficients for the intercept, the central bias, and salience were significantly different from zero, as would be expected from the results of the main GLMM (Table 3).

Tables

Table 1. Individual demographic and clinical data for the AMD patients included in the study.

Participant Number	Gender	Age	MMSE score	Duration of AMD (months)	Visual acuity (LogMAR)	GLD (mm)	SA (mm^2)	BCEA ($minarc^2$)
1	female	82	27	42.4	0.6	3.417	6.97	3120.71
2	female	78	28	45.7	0.4	3.058	4.8	2340.08
3	female	82	30	76.1	0.4	2.925	4.91	3253.23
4	female	72	30	74.2	1	3.375	8.9	8779.51
5	female	80	29	13.8	0.8	3.532	9.57	5555.60
6	male	83	28	14.4	0.4	2.586	2.82	1883.36
7	female	80	30	3	1.6	6.525	25.74	11394.56
8	female	78	28	27.3	0.4	1.623	1.39	16657.36
9	female	77	30	7.5	0.6	2.831	4.21	1349.14
10	female	81	30	73.2	1	5.896	21.21	13908.58
11	female	79	30	7.9	0.4	0.384	0.04	13542.71
12	female	71	29	9.1	0.3	1.758	2.83	17492.23
13	female	81	30	60	0.8	4.910	9.79	16903.14
14	male	86	30	41	0.3	0.855	0.42	9249.95
15	female	74	27	1.8	0.7	3.006	5.3	11162.78
16	female	73	30	98	0.4	2.669	3.64	900.34
17	male	73	26	41	0.9	4.681	10.65	11057.94

Note. MMSE = Mini Mental State Examination, AMD = age-related macular degeneration, LogMAR = logarithm of the minimum angle of resolution, GLD = greatest linear diameter of the lesion, SA = surface area, BCEA = bivariate contour ellipse area.

Table 2. Mean (and standard deviation) general scanning behavior per participant for AMD patients, age-matched normally sighted subjects, and young adults.

		Number of fixations per trial	Fixation duration (ms)	Saccade amplitude (°)
Subject group	AMD patients	30.35 (9.1)	233.93 (97.3)	3.18 (1.05)
	older adults	30.52 (5.61)	241.46 (64.38)	4.6 (1.19)
	young adults	29.5 (5.37)	270 (84.79)	5.1 (1.25)

Table 3. Generalized linear mixed model fitting the effect of image salience and central bias on fixation probability in scene viewing: estimates of coefficients (*b*), standard errors (*SE*), *z*-values, and *p*-values for fixed effects and variances and correlations for random effects.

Fixed Effects	*B*	*SE*	*z*	*p*
Intercept (Old)	-2.0495	0.1218	-16.827	< 0.001
Intercept: AMD - Old	-0.8298	0.1645	-5.045	< 0.001
Intercept: Young - Old	0.2911	0.162	1.797	0.072
Central bias (Old)	-0.772	0.0944	-8.175	< 0.001
Central bias: AMD - Old	-0.534	0.1282	-4.165	< 0.001
Central bias: Young - Old	0.2561	0.1263	2.028	0.043
Salience (Old)	0.245	0.072	3.401	0.001
Salience: AMD - Old	-0.0077	0.0797	-0.097	0.923
Salience: Young - Old	0.2497	0.0787	3.171	0.002
Random Effects				
Groups	Name	Variance	Correlation	
Subject	Intercept	0.21583	Intercept	
	Central bias	0.12932	0.74	Central bias
	Salience	0.04866	-0.11	-0.15
Scene	Intercept	0.03314	Intercept	
	Central bias	0.01780	0.50	Central bias
	Salience	0.04069	0.25	0.43